Published in final edited form as:
Cancer Res. 2010 March 1; 70(5): 1854–1865. doi:10.1158/0008-5472.CAN-09-1922.

Reexpression of hSNF5 in malignant rhabdoid tumor cell lines causes cell cycle arrest through a p21$^{CIP1/WAF1}$-dependent mechanism

Yasumichi Kuwahara[1], **Aubri Charboneau**[1], **Erik S. Knudsen**[2], and **Bernard E. Weissman**[1,*]

[1]Department of Pathology and Laboratory Medicine, UNC Lineberger Comprehensive Cancer Center, University of North Carolina at Chapel Hill, Chapel Hill, North Carolina 27599

[2]Department of Cell Biology, Kimmel Cancer Center, Thomas Jefferson University, Philadelphia, PA 19107

Abstract

Loss of hSNF5 function is usually observed in malignant rhabdoid tumor (MRT), a highly aggressive pediatric neoplasm. Previous studies have shown that reexpression of hSNF5 in MRT cell lines causes G_1 cell cycle arrest with *p16^{INK4A}*, *p21$^{CIP1/WAF1}$* and *cyclin D_1* playing key roles in MRT cell growth control. However, we have shown that reexpression of hSNF5 induced cell cycle arrest in the absence of p16^{INK4A} expression. These results indicate that the mechanism of hSNF5-induced cell cycle arrest is context dependent. Here, we investigated the relationship between p21$^{CIP1/WAF1}$ and hSNF5 in the regulation of growth using several MRT cell lines. We found that G_1 cell cycle arrest occurred concomitant with an increase in *p21$^{CIP1/WAF1}$* mRNA and protein levels and preceeded *p16^{INK4A}* mRNA and protein up-regulation. Chromatin immunoprecipitation data confirmed that hSNF5 appeared at both p21$^{CIP1/WAF1}$ and p16^{INK4A} promoters after reexpression. We further showed that p21$^{CIP1/WAF1}$ induction showed both p53 dependent and independent mechanisms. We also demonstrated that reduction of p21$^{CIP1/WAF1}$ expression by RNAi significantly inhibited hSNF5-induced G_1 arrest. Our results demonstrate that both p21$^{CIP1/WAF1}$ and p16^{INK4A} are targets for hSNF5, and that p21$^{CIP1/WAF1}$ up-regulation during hSNF5-induced G_1 arrest precedes p16^{INK4A} up-regulation. These findings indicate that SNF5 mediates a temporally controlled program of CDK inhibition to restrict aberrant proliferation in MRT cells.

Keywords

SNF5/INI1; p21$^{WAF1/CIP1}$; p16^{INK4A}; chromatin remodeling

Introduction

Malignant rhabdoid tumor (MRT) is a rare and extremely aggressive childhood cancer. MRT was initially described as an unfavorable histologic type of pediatric renal tumor, a variant of Wilms' tumor (1). While the most common locations occur in the kidney and central nervous system, MRT also arise in almost any site (2,3). Despite significant advances in the treatment and outcome of other pediatric tumors, for MRTs diagnosed before the age of 6 months, patient survival at 4 years drops to approximately 8.8% (4). Therefore, improved patient outcome

*Corresponding Author. **Mailing address:** UNC Lineberger Comprehensive Cancer Center, University of North Carolina, CB#7259, Room 32-048, Chapel Hill, NC 27599-7295. Phone: (919) 966-7533.Fax: (919) 966-7533. weissman@med.unc.edu

requires a better understanding of malignant rhabdoid tumorigenesis and the development of novel therapeutic strategies.

In the past several years, the discovery of deletions and mutations at 22q11.2 involving *hSNF5/INI1* has contributed to the clarification of pathogenesis of MRT (5). The finding that genetic alterations in MRTs are usually limited to *hSNF5* mutations and deletions implicates the loss of hSNF5 function as the primary cause of these tumors. Now, hSNF5 function is recognized as being lost in almost 100% of MRTs (6,7). Therefore, the elucidation of hSNF5 function should lead to the identification of the key molecular steps necessary for MRT tumorgenesis.

hSNF5 is one of the core subunits of the SWI/SNF chromatin remodeling complex that also includes an ATPase subunit (either BRG1 or BRM), BAF155, and BAF170. SWI/SNF complexes are ATP-dependent chromatin remodeling complexes that regulate gene transcription by causing conformational changes in chromatin structure, as well as by cooperation with histone acetylation complexes (8). In human cells, studies have shown a role for transcriptional regulation by SWI/SNF complexes in the control of cell growth, tissue differentiation, and embryo development in multiple tissues (9). Furthermore, loss of BRG1 function has been observed in malignant tumors including lung, pancreatic, breast, and prostate cancer (10-13). Several new SWI/SNF members, such as BAF180, have been found to form different subsets of SWI/SNF complexes with distinct functions (14-16). To understand how the SWI/SNF complex regulates gene expression in a complex and precise manner has become increasingly important.

Recently, several reports have shown that hSNF5 plays key roles in cell cycle control, differentiation, and oncogenic transformation. Reexpression of hSNF5 induces G_1 cell cycle arrest in MRT cell lines, accompanied by up-regulation of $p16^{INK4A}$ and down-regulation of cyclin D_1, cyclin A, and phosphorylated retinoblastoma protein (pRb), suggesting a key role for these genes in MRT cell cycle control (17-20). Kia *et al.* reported reexpression of hSNF5 mediates eviction of polycomb complex proteins such as BMI-1 from epigenetically silenced promoters of the *INK4b-ARF-INK4a* locus followed by their activation (21). Furthermore, some reports demonstrated that hSNF5 controls the differentiation of MRT cells (22,23) and hSNF5 loss changes gene transcription epigenetically and contributes to oncogenesis without genomic instability (24).

Our previous study showed that reexpression of hSNF5 induced cell cycle arrest even in the absence of $p16^{INK4A}$ expression (25). This finding suggested that other genes besides $p16^{INK4A}$ play a critical role at early time points of G_1 cell cycle arrest induced by hSNF5. Therefore, in this study, we determined the mechanism of G_1 cell cycle arrest induced by hSNF5 in MRT cells within 24 hours after reexpression using adenoviral vectors. We show that induction of $p21^{WAF1/CIP1}$ appears at the onset of hSNF5-induced growth arrest and precedes $p16^{INK4A}$ expression. Furthermore, we demonstrate that $p21^{WAF1/CIP1}$ knock-down inhibits hSNF5-induced G_1 cell cycle arrest. We also show differences in the histone methylation changes at these 2 promoters after hSNF5 reexpression. Finally, we demonstrate that $p21^{WAF1/CIP1}$ shows both p53 dependent and independent mechanisms of induction after hSNF5 reexpression. Our results suggest that $p21^{WAF1/CIP1}$ plays a key role in hSNF5 control of cell growth, and hSNF5 loss may alter $p21^{WAF1/CIP1}$ transcription by a different mechanism than that reported for the $p16^{INK4A}$ promoter in MRT cells.

Materials and Methods

Cell culture and adenovirus infection

A204.1 (ATCC), G401.6 (ATCC), TTC642 (Dr. Timothy Triche- Childrens Hospital of Los Angeles), and NIH3T3 (Dr. Stuart Aaronson-National Cancer Institute) cells were cultured in

RPMI 1640 medium and UNC N3T cells in bronchial epithelial growth medium (BEGM) (26). 293FT cells were cultured in DMEM medium containing 10% fetal bovine serum. The Ad/pAdEasyGFPINI-SV^{+} adenoviral vectors expressing hSNF5 and co-expressing the green fluorescent protein (GFP) (designated Ad-hSNF5) and the Ad/pAdEasyGFP expressing GFP (designated Ad-GFP) were previously published (20). In order to achieve infection of over 90% cells, we infected at a multiplicity of infection (M.O.I.) of 20 for the A204.1 cell line and 200 for the TTC642 cell line.

Protein extracts and Western blotting

Western blotting was carried out as described previously (25). Western analyses of proteins were carried out by using anti-p21$^{CIP1/WAF1}$ (AB1; Calbiochem), anti-p16^{INK4a} (G175-1239; BD Pharmingen), anti-pRb (G3-245; BD Pharmingen), anti-actin (A2066; Sigma), anti-p53 (DO-1; Santa Cruz), anti–cyclin A (H-432; Santa Cruz Biotechnology), anti-hSNF5 (BD Transduction Laboratories), BMI-1 (upstate cloneF6; Millipore), and horseradish peroxidase–conjugated anti-rabbit or anti-mouse IgG (GE Healthcare).

RNA extraction and Quantitative real-time reverse transcription-PCR analysis

RNA was extracted using the RNeasy mini kit (Qiagen), and 1 μg was used for cDNA synthesis primed with Random Primers (Invitrogen). cDNA was analyzed using TaqMan (Applied Biosystems) quantitative real-time reverse transcription-PCR (QT-PCR) analysis with *β-actin* as the reference gene in each reaction. Reactions were performed on an ABI 7900 HT sequence detection system (Applied Biosystems) and relative quantification was determined using the $2^{-\Delta\Delta Ct}$ method (27). The primers used for p16^{INK4a} QT-PCR were 5′-CTGCCCAACGCACCGAATA-3′ and 5′-GCGCTGCCCATCATCATGA-3′. The probe used for p16^{INK4a} QT-PCR was 5′-CTGGATCGGCCTCCGACCGTA-3′. The TaqMan gene expression assay primer/probe set (Hs00355782_m1; Applied Biosystems) was used for p21$^{CIP1/WAF1}$, the primer/probe set (Hs01034249_m1; Applied Biosystems) was used for p53, and the primer/probe set (Hs99999903_m1; Applied Biosystems) was used for β-actin.

Chromatin immunoprecipitation

Chromatin immunoprecipitation (ChIPs) was carried out as described by Donner et al (28). Immunoprecipitation was performed with an antibody specific to hSNF (Dr. Tony Imbalzano), histone H3 trimethylation of lysine 4 (H3K4 me3) (ab8580; Abcam), BRG-1 (J1; Dr. Weidong Wang), BMI-1 (upstate cloneF6; Millipore), normal Rabbit IgG (sc-2027; Santa Cruz Biotechnology), normal mouse IgG (sc-2025; Santa Cruz Biotechnology) or p53 (DO-1; Calbiochem). DNA present in each IP was quantified by QT-PCR using gene-specific primers on an ABI 7000 sequence detection system. All expression values were normalized against input DNA. Antibody specificity was also determined for each cell line (Supplementary Figure 1). The primer sequences are shown in Supplementary Table 1.

Lentiviral procedures and shRNA

Lentivirus was generated using 293FT cells following the protocol of Kafri and co workers (29). Either pLKO.1, a non-target shRNA control vector (SHC002; Sigma), an equal mixture of 5 types of NM_00039 p21 MISSION shRNA Lentiviral Transduction Particles (TRCN0000040123, TRCN0000040124, TRCN0000040125, TRCN0000040126 and TRCN0000040127) or NM_000546 p53 MISSION shRNA Lentiviral Transduction Particles (TRCN0000003756), obtained from Sigma, were co-transfected with the packing construct ΔNRF (from Dr. Tal Kafri, The University of North Carolina) (29), and the VSV-G envelope expression plasmid (pMDK64; from Dr. Matthias Kaeser, The Salk Institute) into 293FT cells with FuGene® (Roche). pLKO.1 is a negative control containing an insert sequence that does not target any human or mouse gene, but will activate the RNAi pathway. For infection, cells

were incubated with lentiviral particles and polybrene and then selected with puromycin. At least 3 puromycin-resistant colonies of the A204.1 and TTC642 cells were isolated and expanded for further characterization.

Cell cycle analysis

Cell cycle analyses were performed according to the procedure of Huang S *et al.* (30). Percentages of cells within each of the cell cycle compartments were determined by flow cytometry (CyAn; Dako) and analyzed with ModFit software (Verity).

Results

The effects of reexpression of hSNF5 on the growth of MRT cell lines

We have previously shown that both hSNF5 and $p16^{INK4A}$ can induce G_1 cell cycle arrest in MRT cell lines at 72 hours after transfection (19). However, hSNF5 also induced G_1 cell cycle arrest without $p16^{INK4A}$ induction in the same timeframe (25). Because of the extended period between hSNF5 transfection and the characterization of cell cycle arrest in these previous studies, we characterized the effects of hSNF5 expression on the growth of 2 MRT cell lines within 24 of infection with Ad-hSNF5 and Ad-GFP (negative control) adenoviruses.

The induction of hSNF5 protein expression in the A204.1 and TTC642 cells by adenoviral infection is shown in Figure 1A. No hSNF5 expression was detected in either MRT cell line in the absence of infection or after Ad-GFP infection. However, infection with Ad-hSNF5 led to hSNF5 expression as early as 12 hours post-infection, followed by a time-dependent increase in hSNF5 expression levels in both MRT cells lines.

We next tested the effects of hSNF5 reexpression on cell cycle regulation by flow cytometry. Both cell lines infected with Ad-hSNF5 showed cell cycle arrest 24 hours after infection, characterized by the presence of nearly 80% of cells in the G_1 phase of the cell cycle and the presence of <10% of cells in the S phase (Fig. 1B). The percentage of Ad-hSNF5- and Ad-GFP-infected cells in S phase was significantly different at 24 hours after infection. Similar results were found at 48 hours post-infection. These results demonstrated that the G_1-S cell cycle progression was inhibited by 24 hours after hSNF5 reexpression in these MRT cell lines.

hSNF5-induced $p16^{INK4A}$ and $p21^{CIP1/WAF1}$ protein expression in MRT cell lines

We previously demonstrated that hSNF5 reexpression induced the down-regulation of Cyclin A, the dephosphorylation of pRb, and up-regulation of $p16^{INK4A}$ and $p21^{CIP1/WAF1}$ expression at 3 days following transfection (25). To determine whether these changes also occurred simultaneously with hSNF5-induced cell cycle arrest at 24 hours post-infection, we examined the expression of cyclin dependent kinase (CDK) inhibitors, especially $p16^{INK4A}$ and $p21^{CIP1/WAF1}$, as well as their downstream targets by western blotting (Fig. 1C). We observed increased $p21^{CIP1/WAF1}$ and decreased phosphorylated-pRb and cyclin A levels at 24 hours after Ad-hSNF5 infection compared to Ad-GFP control and un-infected control in both A204.1 and TTC642 cells. In the A204.1, $p16^{INK4A}$ protein levels were increased slightly at 12 hours after Ad-hSNF5 infection, and showed a further increase at 24 hours after infection compared to control cells. In contrast, $p16^{INK4A}$ protein expression was absent at baseline in the TTC642, with a slight increase at 24 hours, followed by a marked increase at 48 hours after infection. On the other hand, p53 was not significantly changed in both MRT cell lines (Fig. 1C).

Reexpression of hSNF5 induces *$p21^{CIP1/WAF1}$* transcription with or without p53 recruitment in MRT cell lines

We next examined whether the increase in $p21^{CIP1/WAF1}$ protein levels resulted from an increase in its mRNA levels by QT-PCR. We found the level of *$p21^{CIP1/WAF1}$* mRNA increased

within 12 hours after Ad-hSNF5 infection in comparison with Ad-GFP infection in both MRT cell lines. In the TTC642, *p21*$^{CIP1/WAF1}$ also increased more with Ad-GFP infection than un-infected control, especially at 48 hours (Fig. 2A).

In our previous study, we showed hSNF5 regulated *p21*$^{CIP1/WAF1}$ and *p16*^{INK4A} transcription in A204.1 at 4 days after hSNF5 plasmid transfection by ChIPs (25). Therefore, we analyzed the chromatin status at *p21*$^{CIP1/WAF1}$ promoter, −2283 kb (p53 high-affinity binding site) and −1391 kb (p53 low-affinity binding site) in both A204.1 and TTC642 cells (28), at 24 hours after Ad-hSNF5 infection to clarify the mechanism of *p21*$^{CIP1/WAF1}$ activation by hSNF5. ChIPs data confirmed that hSNF5 bound to both −2283 kb site and −1391 kb site in either cell line. Furthermore BRG1 is also recruited by hSNF5 induction to both sites in A204.1, but only at the −2283 site in TTC642 (Fig. 2B).

Moreover, our previous reports also suggested hSNF5 recruits p53 to the p21 promoter (25). Therefore, we determined whether hSNF5 recruitment to the p21 promoter affected p53 binding. In A204.1, p53 binding is increased after hSNF5 reexpression, with a higher amount detected at the high affinity −2283 kb site (Fig. 2B). In contrast, we did not observe a difference in p53 recruitment between Ad-hSNF5 infection and Ad-GFP infection in the TTC642 although the difference in binding between the 2 affinity sites remained (Fig. 2B). We next determined the effect of hSNF5 reexpression on the H3K4me3, a chromatin mark associated with gene activation (31). H3K4me3 decreased after hSNF5 reexpression at both the −2283 kb and −1391 kb sites in both the A204.1 and TTC642 cells (Fig. 2B).

Reexpression of hSNF5 induces *p21*$^{CIP1/WAF1}$ transcription through both p53-dependent and p53-independent mechanisms in MRT cell lines

Because our results indicated that hSNF5 reexpression activated *p21*$^{CIP1/WAF1}$ transcription with p53 recruitment in A204.1 cells but without p53 recruitment in TTC642 cells, we next assessed the role of p53 in *p21*$^{CIP1/WAF1}$ transcription in the MRT cell lines. We established 2 independently derived p53 stable knock-down MRT cell lines from both A204.1 and TTC642 cells using lentiviral vectors encoding a small hairpin RNA (shRNA) targeting *p53* mRNAs. We also developed a negative control cell line using a lentiviral vector encoding a small hairpin RNA targeting a non-mammalian sequence (pLKO.1). By QT-PCR and Western blotting, all p53 knock-down cells (A204.1 p21KD and TTC642 p21 KD) showed significant decreases in the p53 mRNA levels along with the protein levels of p53 and p21$^{CIP1/WAF1}$ compared with the parental cells or the control cells (A204.1 pLKO.1 and TTC642 pLKO.1) (Fig. 3A).

We next determined whether the reduction in p53 expression affected *p21*$^{CIP1/WAF1}$ transcription induced by hSNF5. Infection of the pLKO.1 and p53KD cells with Ad-hSNF5 or Ad-GFP resulted in increased levels of *p21*$^{CIP1/WAF1}$ mRNA at 24 hours after Ad-hSNF5 infection in pLKO.1 cells as in the parental cell lines (Fig.3B). However, while the increase of *p21*$^{CIP1/WAF1}$ mRNA by hSNF5 reexpression was significantly inhibited in all A204.1 p53KD cells, the increase of *p21*$^{CIP1/WAF1}$ mRNA by hSNF5 reexpression was not significantly different among TTC642, TTC642 pLKO.1 and all TTC642 p53KD cells (Fig. 3B). These results suggested that the up-regulation p21$^{CIP1/WAF1}$ transcription by hSNF5 reexpression was operated through p53-dependent mechanism in A204.1 cells and through a p53-independent mechanism in TTC642 cells.

Reexpression of hSNF5 induces *p16*^{INK4A} transcription through BMI-1 eviction in the TTC642 cell line

Although the A204.1 expresses p16^{INK4A} mRNA and protein, the TTC642 does not show detectable expression of p16^{INK4A} protein. However, reexpression of hSNF5 caused up-regulation of p16^{INK4A} protein in both MRT cell lines (Fig. 1C). We, therefore, examined

whether the increase of $p16^{INK4A}$ protein resulted from an increase in its mRNA levels by QT-PCR. We found that *p16*^{INK4A} mRNA levels increased within 24 hours and 48 hours after Ad-hSNF5 infection in the A204.1 and in TTC642 cells, respectively (Fig. 4A). These results demonstrated the increase in $p21^{CIP1/WAF1}$ mRNA occurs earlier than the increase in $p16^{INK4A}$ mRNA.

Because BMI-1 represses transcription at *p16*^{INK4A} locus (32) and an earlier report indicated that *p16*^{INK4A} transcription is activated by induction of hSNF5 via BMI-1 eviction (21), we first confirmed that hSNF5 binding at the *p16*^{INK4A} promoter increased at 24 hours after Ad-hSNF5 infection in both cell lines (Fig. 4B). We next determined the binding of BMI-1 to the *p16*^{INK4A} promoter as an indication of polycomb complex silencing. In TTC642, we observed BMI-1 binding was also significantly less after infection of Ad-hSNF 24 and 48 hours after infection compared with control infected cells (Fig. 4B). We also found a modest increase in BRG-1 binding on the *p16*^{INK4A} promoter after hSNF5 reexpression at 24 hours followed by a dramatic increase in H3K4 me3 binding at 48 hours in TTC642 cells (Fig. 3B, 3C). These results appear consistent with hSNF5 reexpression increasing the binding of the SWI/SNF complex to the *p16*^{INK4A} promoter accompanied by polycomb eviction at 24 hours followed by H3K4 methylation, and activation of *p16*^{INK4A} transcription at 48 hours in TTC642 cells.

In contrast, we detected little BMI-1 binding on the *p16*^{INK4A} promoter in A204.1 cells, even in the absence of hSNF5 expression (Fig. 4B). We also observed that hSNF5 reexpression had little effect on the binding of BRG-1 and the level of H3K4 methyation at this promoter (Fig. 4B, C). These results suggested an absence of polycomb complex silencing at the *p16*^{INK4A} promoter in the A204.1 cells. Therefore, we examined the expression of BMI-1 in our MRT cell lines by Western blotting. The results in Figure 4F demonstrate that the A204.1 cell line fails to express detectable BMI-1 protein compared to the TTC642 cell line (Fig. 4D). The absence of BMI-1 may explain the basal level of *p16*^{INK4A} mRNA observed in A204.1 cells.

Reduced $p21^{CIP1/WAF1}$ expression inhibits the G_1 arrest induced by re-expression of hSNF5 in MRT cell lines

Because our results indicated that hSNF5 reexpression activated *p21*$^{CIP1/WAF1}$ transcription earlier than *p16*^{INK4A} transcription, we next assessed the role of $p21^{CIP1/WAF1}$ in hSNF5-induced cell cycle arrest in the MRT cell lines. We established 3 independently derived $p21^{CIP1/WAF1}$ stable knock-down MRT cell lines from both A204.1 and TTC642 cells using lentiviral vectors encoding a small hairpin RNA (shRNA) targeting *p21*$^{CIP1/WAF1}$ mRNAs and a negative control cell line (pLKO.1). By QT-PCR and Western blotting, all $p21^{CIP1/WAF1}$ knock-down cells (A204.1 p21KD and TTC642 p21 KD) showed significant decreases in the mRNA levels along with the protein levels of $p21^{CIP1/WAF1}$ compared with the parental cells or the control cells (A204.1 pLKO.1 and TTC642 pLKO.1) (Fig. 5A).

We next determined whether the reduction in $p21^{CIP1/WAF1}$ expression affected hSNF5 induced cell cycle arrest. Therefore, we infected the pLKO.1 and p21KD cells with Ad-hSNF5 or Ad-GFP, and assayed the effects on cell cycle by flow cytometry. We observed a similar G_1 cell cycle arrest induced by Ad-hSNF5 infection in pLKO.1 cells after 24 hours as in the parental cell lines (Fig. 5B). However, the inhibition of the G_1-S cell cycle progression by hSNF5 reexpression was significantly inhibited in all A204.1 p21KD cells and TTC642 p21KD cells (Fig. 5B). These results indicated that $p21^{CIP1/WAF1}$ up-regulation contributes to the inhibition of the G_1-S cell cycle progression by hSNF5 at 24 hours after Ad-hSNF5 infection.

Reduced p21$^{CIP1/WAF1}$ expression inhibits the dephosphorylation of pRb after hSNF5 reexpression in MRT cell lines

Because p21$^{CIP1/WAF1}$ knock-down caused inhibition of G_1 cell cycle arrest induced by hSNF5 reexpression, we examined whether the effect occurred at the level of pRb phosphorylation. Although p21$^{CIP1/WAF1}$ expression increased after hSNF5 reexpression in A204.1 pLKO.1 and TTC642 pLKO.1 cell lines, we observed limited increase of p21$^{CIP1/WAF1}$ and limited reduction of phosphorylated-pRb and cyclin A at 24 hours after Ad-hSNF5 infection in A204 p21KD cells and TTC642 p21KD cells (Fig. 6A & B). The expression of p16^{INK4A} was not significantly increased at 24 hours after Ad-hSNF5 infection in A204.1 p21KD cells. In TTC642 p21KD cells, the p16^{INK4A} protein increased slightly at 24 hours after Ad-hSNF5 infection (data not shown), then increased significantly at 48 hours, similar to the TTC642 parent cell line (data not shown). The change of p21$^{CIP1/WAF1}$ mRNA was similar to the results seen with p21$^{CIP1/WAF1}$ protein levels (data not shown). Taken together, these results indicated that the G_1 arrest induced by hSNF5 reexpression strongly correlated with dephosphorylation of pRb through p21 $^{CIP1/WAF1}$ activation.

Discussion

By studying the mechanism of G_1 cell cycle arrest induced by hSNF5 at a time point concomitant with the induction of growth arrest, our study shows three important observations. First, hSNF5 directly regulates the p21$^{CIP1/WAF1}$ and p16^{INK4A} loci through different mechanisms among MRT cell lines. Second, hSNF5 can regulates the p21$^{CIP1/WAF1}$ through either a p53-dependent or a p53-independent mechanism. Finally, p21$^{CIP1/WAF1}$ has a key role in hSNF5-induced cell growth arrest in MRT cell lines.

Reexpression of hSNF5 increased p21$^{CIP1/WAF1}$ transcriptional activity immediately through the recruitment of BRG1 to the p21$^{CIP1/WAF1}$ promoter. Similarly, some reports have suggested that BRG1 associates with the p21$^{CIP1/WAF1}$ promoter and activates it along with hSNF5 (33,34). Does this recruitment of the SWI/SNF complex lead to an interaction with another transcription factor? Lee *et al.* (35) suggested that the BRG-1 interacts with p53 and activates the p21$^{CIP1/WAF1}$ promoter in a p53-dependent manner. In contrast, Liu *et al.* (36) and Hendricks *et al.* (33) suggested that BRG-1 activates the p21$^{CIP1/WAF1}$ promoter in p53-independent manner. Indeed, previous reports have shown that multiple mechanisms can activate the p21$^{CIP1/WAF1}$ promoter including p53-dependent, Sp1- or Sp3-dependent, or CDK8-dependent (37). Our results in the A204.1 cell line appear consistent with the former model. We observed increased p53 levels at the p21$^{CIP1/WAF1}$ promoter after hSNF5 reexpression and reduction in p53 expression inhibited up-regulation of p21$^{CIP1/WAF1}$ induced by hSNF5. This finding, at a minimum, supports the notion that reexpression of hSNF5 in these cells facilitates the recruitment of p53 to the p21$^{CIP1/WAF1}$ promoter. However, our studies did not determine whether this occurs through a direct interaction between p53 and hSNF5. We also need to identify the upstream signal that initiates p53 binding to the p21$^{CIP1/WAF1}$ promoter.

In contrast, p53 levels on p21$^{CIP1/WAF1}$ did not change in the TTC642 cells after hSNF5 reexpression nor did decreased p53 levels affect the ability of hSNF5 to increase p21$^{CIP1/WAF1}$ transcription. While we cannot exclude the possibility that a low level of p53 protein remains at the p21$^{CIP1/WAF1}$ promoter, sufficient for transcriptional activation, it appears that hSNF5 reexpression may operate through a different mechanism in these cells. While activation of p21$^{CIP1/WAF1}$ transcription by hSNF5 in both cell lines appears associated with recruitment of BRG-1, the transcription factors recruited to the p21$^{CIP1/WAF1}$ promoter may differ. Additional ChIPs analyses of the p21$^{CIP1/WAF1}$ promoter in the TTC642 cell line will clarify this matter. In addition, our result showed a modest increase in p21$^{CIP1/WAF1}$ transcription after Ad-GFP infection compared to the uninfected control. We believe that the

high M.O.I. of adenovirus required for infection of this cell line caused up-regulation of $p21^{CIP1/WAF1}$ through apoptotic induction (38).

We also showed that reexpression of hSNF5 increases $p16^{INK4A}$ transcriptional activity after $p21^{CIP1/WAF1}$ up-regulation. In TTC642 cell line, hSNF5 expression caused decrease of BMI-1 and increase of BRG-1 at the $p16^{INK4A}$ promoter. The level of BMI-1 at 48 hours was less than that at 24 hours, and the decrease of BMI-1 was correlated with an increase of H3K4me3. These results concur with the Kia et. al. report showing hSNF5 induced a decrease of BMI-1 and an increase of H3K4me3 on the $p16^{INK4A}$ promoter, and that BRG1 was necessary for activation of the $p16^{INK4A}$ promoter by hSNF5 (21). On the other hand, the A204.1 cell line expresses low basal levels of $p16^{INK4A}$ consistent with a lack of expression of BMI-1. Our results appear in accord with the report that $p16^{INK4A}$ expression is directly regulated by polycomb proteins such as BMI-1 and EZH2 (39). Moreover, while hSNF5 appeared at $p16^{INK4A}$ promoter after reexpression followed by an increase in $p16^{INK4A}$ mRNA in the A204.1 cell line, BRG-1 and H3K4me3 levels at the promoter did not change significantly. Therefore, in the absence of polycomb silencing, $p16^{INK4A}$ mRNA could increase more rapidly in the A204.1 cell line than in the TTC642 cell line. Regardless, the data still show that the hSNF5-induced increase in $p16^{INK4A}$ levels in the A204.1 cell line follows the $p21^{CIP1/WAF1}$ up-regulation regardless of BMI-1 expression. The mechanism for the increase in $p16^{INK4A}$ mRNA in the A204.1 cell line requires further investigation.

The difference in H3K4me3 patterns between the $p21^{CIP1/WAF1}$ and $p16^{INK4A}$ promoters was unexpected. The significant increase in H3K4me3 at the $p16^{INK4A}$ promoter (−450 kb) in the TTC642 cell line after hSNF5 reexpression appears consistent with the activation of transcription from this promoter. Although the levels of this modification did not change in the A204.1 cell line, this may reflect the active $p16^{INK4A}$ transcription present in these cells before hSNF5 reexpression. However, in both cell lines, H3K4me3 decreased at the p53 binding sites in the $p21^{CIP1/WAF1}$ promoter (−2283 kb and −1391 kb) after hSNF5 reexpression, even though $p21^{CIP1/WAF1}$ transcription increased. One possible explanation for this observation might come from hSNF5 reexpression activating SWI/SNF complex activity resulting in nucleosome repositioning by chromatin remodeling. Therefore, the subsequent change in H3K4me3 positioning on the $p21^{CIP1/WAF1}$ promoter would be reflected by a decreased signal in our ChIPs assay.

In our study, $p21^{CIP1/WAF1}$ knock-down experiments showed that inhibition of $p21^{CIP1/WAF1}$ expression partially inhibited the efficiency of hSNF5-induced G_1 cell cycle arrest in MRT cell lines. The failure to completely abrogate the growth arrest may result from the residual activation of $p21^{CIP1/WAF1}$ protein in the RNAi-expressing MRT cell lines. In addition, the increasing levels of $p16^{INK4A}$ protein may also begin to affect the cells because we observed a complete cell cycle arrest at 48 hours in the p21 knock-down cells (unpublished observations). We also cannot exclude the possibility that altered expression of other cell cycle regulatory genes may contribute the G1 arrest induced by hSNF5 (40,41). This result indicated that $p21^{CIP1/WAF1}$ has a key role in hSNF5-induced cell growth arrest in MRT cell lines. Importantly, Smith et al. recently showed cell cycle arrest and cytotoxicity induced by flavopiridol in MRT cell lines correlated with the down-regulation of cyclin D1 and the up-regulation of $p21^{CIP1/WAF1}$ (42). Taken together, these results support $p21^{CIP1/WAF1}$ as a relevant target for therapy of MRT.

Many MRTs arise under in infants under the age of 6 months and in neonates (43). Therefore, it seems plausible that a significant number of MRTs arise from the loss of hSNF5 in stem cells or progenitor cells during development. The expression of $p16^{INK4A}$ in stem cells is restricted by the expression of BMI-1 (44). Indeed, mouse embryo cells do not display expression of $p16^{INK4A}$ (45) and stem cells in young mice (8-12 week old) do not express

detectable *p16*^{INK4A} mRNA (46). Thus, a strong possibility exists that p16^{INK4A} was already silenced in the cell that gave rise to the TTC642 cell line before hSNF5 loss occurred.

Our results may indicate that a decrease in p21$^{CIP1/WAF1}$ expression following hSNF5 loss may signify one key event during MRT development. For example, the absence of p21$^{CIP1/WAF1}$ expression can increase hematopoietic stem cell proliferation (47) or maintain neural stem cells by playing a significant role in regulating their proliferation (48). Our recent studies showing cooperation between SNF5 loss and pRb family inactivation in the acceleration of formation of spinal cord MRTs in mice support this notion (49). These results suggest that p21$^{CIP1/WAF1}$ and its down-stream targets may regulate the boundary between quiescence and proliferation in stem cells and progenitor cells.

In conclusion, our results demonstrated that while hSNF5 reexpression in MRT cells increases both p21$^{CIP1/WAF1}$ and p16^{INK4A} expression during the induction of G_1 cell cycle arrest, p21$^{CIP1/WAF1}$ up-regulation precedes p16^{INK4A}. While our studies firmly substantiate p21$^{CIP1/WAF1}$ as a key target for hSNF in cell cycle regulation, the role of hSNF5 within the activities of SWI/SNF complex and gene regulation appear complex. Studies from other laboratories also implicate a role for hSNF5 the regulation cellular differentiation, cell migration and DNA repair (40,41,50). However, the establishment that SNF5 loss alters p21$^{CIP1/WAF1}$ expression during MRT tumorigenesis provides an important new target for therapy in a tumor with limited options for treatment.

Supplementary Material

Refer to Web version on PubMed Central for supplementary material.

Acknowledgments

We thank Dr. Matthias Kaeser for his excellent technical input and thoughtful discussions, Dr. Cindy Wright, Medical University of South Carolina, for the Ad-SNF5 and Ad-GFP reagents, Dr. Scott Randell, University of North Carolina, for the UNC N3T cell line and Dr. Tony Imbalzano, University of Massachusetts School of Medicine, for the SNF5 antiserum.

This work was supported by Public Health Service grants CA91048 (BEW) and R01-CA104213 (ESK) from the National Cancer Institute and the American Brain Tumor Association Chad Dunbar Postdoctoral Fellowship (AC).

References

1. Beckwith JB, Palmer NF. Histopathology and prognosis of Wilms tumors: results from the First National Wilms' Tumor Study. Cancer 1978;41:1937–48. [PubMed: 206343]
2. Hoot AC, Russo P, Judkins AR, Perlman EJ, Biegel JA. Immunohistochemical analysis of hSNF5/INI1 distinguishes renal and extra-renal malignant rhabdoid tumors from other pediatric soft tissue tumors. Am J Surg Pathol 2004;28:1485–91. [PubMed: 15489652]
3. Biegel JA, Tan L, Zhang F, Wainwright L, Russo P, Rorke LB. Alterations of the hSNF5/INI1 gene in central nervous system atypical teratoid/rhabdoid tumors and renal and extrarenal rhabdoid tumors. Clin Cancer Res 2002;8:3461–7. [PubMed: 12429635]
4. Tomlinson GE, Breslow NE, Dome J, et al. Rhabdoid tumor of the kidney in the National Wilms' Tumor Study: age at diagnosis as a prognostic factor. J Clin Oncol 2005;23:7641–5. [PubMed: 16234525]
5. Versteege I, Sevenet N, Lange J, et al. Truncating mutations of hSNF5/INI1 in aggressive paediatric cancer. Nature 1998;394:203–6. [PubMed: 9671307]
6. Biegel JA, Kalpana G, Knudsen ES, et al. The role of INI1 and the SWI/SNF complex in the development of rhabdoid tumors: meeting summary from the workshop on childhood atypical teratoid/rhabdoid tumors. Cancer Res 2002;62:323–8. [PubMed: 11782395]

7. Rousseau-Merck MF, Fiette L, Klochendler-Yeivin A, Delattre O, Aurias A. Chromosome mechanisms and INI1 inactivation in human and mouse rhabdoid tumors. Cancer Genet Cytogenet 2005;157:127–33. [PubMed: 15721633]
8. Roberts CW, Orkin SH. The SWI/SNF complex--chromatin and cancer. Nat Rev Cancer 2004;4:133–42. [PubMed: 14964309]
9. de la Serna IL, Ohkawa Y, Imbalzano AN. Chromatin remodelling in mammalian differentiation: lessons from ATP-dependent remodellers. Nat Rev Genet 2006;7:461–73. [PubMed: 16708073]
10. Reisman DN, Sciarrotta J, Wang W, Funkhouser WK, Weissman BE. Loss of BRG1/BRM in human lung cancer cell lines and primary lung cancers: correlation with poor prognosis. Cancer Res 2003;63:560–6. [PubMed: 12566296]
11. Rosson GB, Bartlett C, Reed W, Weissman BE. BRG1 loss in MiaPaCa2 cells induces an altered cellular morphology and disruption in the organization of the actin cytoskeleton. J Cell Physiol 2005;205:286–94. [PubMed: 15887247]
12. Decristofaro MF, Betz BL, Rorie CJ, Reisman DN, Wang W, Weissman BE. Characterization of SWI/SNF protein expression in human breast cancer cell lines and other malignancies. J Cell Physiol 2001;186:136–45. [PubMed: 11147808]
13. Wong AK, Shanahan F, Chen Y, et al. BRG1, a component of the SWI-SNF complex, is mutated in multiple human tumor cell lines. Cancer Res 2000;60:6171–7. [PubMed: 11085541]
14. Xia W, Nagase S, Montia AG, et al. BAF180 is a critical regulator of p21 induction and a tumor suppressor mutated in breast cancer. Cancer Res 2008;68:1667–74. [PubMed: 18339845]
15. Xue Y, Canman JC, Lee CS, et al. The human SWI/SNF-B chromatin-remodeling complex is related to yeast rsc and localizes at kinetochores of mitotic chromosomes. Proc Natl Acad Sci U S A 2000;97:13015–20. [PubMed: 11078522]
16. Nie Z, Xue Y, Yang D, et al. A specificity and targeting subunit of a human SWI/SNF family-related chromatin-remodeling complex. Mol Cell Biol 2000;20:8879–88. [PubMed: 11073988]
17. Zhang ZK, Davies KP, Allen J, et al. Cell cycle arrest and repression of cyclin D1 transcription by INI1/hSNF5. Mol Cell Biol 2002;22:5975–88. [PubMed: 12138206]
18. Versteege I, Medjkane S, Rouillard D, Delattre O. A key role of the hSNF5/INI1 tumour suppressor in the control of the G1-S transition of the cell cycle. Oncogene 2002;21:6403–12. [PubMed: 12226744]
19. Betz BL, Strobeck MW, Reisman DN, Knudsen ES, Weissman BE. Re-expression of hSNF5/INI1/BAF47 in pediatric tumor cells leads to G1 arrest associated with induction of p16ink4a and activation of RB. Oncogene 2002;21:5193–203. [PubMed: 12149641]
20. Reincke BS, Rosson GB, Oswald BW, Wright CF. INI1 expression induces cell cycle arrest and markers of senescence in malignant rhabdoid tumor cells. J Cell Physiol 2003;194:303–13. [PubMed: 12548550]
21. Kia SK, Gorski MM, Giannakopoulos S, Verrijzer CP. SWI/SNF mediates polycomb eviction and epigenetic reprogramming of the INK4b-ARF-INK4a locus. Mol Cell Biol 2008;28:3457–64. [PubMed: 18332116]
22. Albanese P, Belin MF, Delattre O. The tumour suppressor hSNF5/INI1 controls the differentiation potential of malignant rhabdoid cells. Eur J Cancer 2006;42:2326–34. [PubMed: 16908131]
23. Caramel J, Medjkane S, Quignon F, Delattre O. The requirement for SNF5/INI1 in adipocyte differentiation highlights new features of malignant rhabdoid tumors. Oncogene 2008;27:2035–44. [PubMed: 17922027]
24. McKenna ES, Sansam CG, Cho YJ, et al. Loss of the epigenetic tumor suppressor SNF5 leads to cancer without genomic instability. Mol Cell Biol 2008;28:6223–33. [PubMed: 18710953]
25. Chai J, Charboneau AL, Betz BL, Weissman BE. Loss of the hSNF5 gene concomitantly inactivates p21CIP/WAF1 and p16INK4a activity associated with replicative senescence in A204 rhabdoid tumor cells. Cancer Res 2005;65:10192–8. [PubMed: 16288006]
26. Fulcher ML, Gabriel SE, Olsen JC, et al. Novel human bronchial epithelial cell lines for cystic fibrosis research. Am J Physiol Lung Cell Mol Physiol 2009;296:L82–91. [PubMed: 18978040]
27. Livak KJ, Schmittgen TD. Analysis of relative gene expression data using real-time quantitative PCR and the 2(-Delta Delta C(T)) Method. Methods 2001;25:402–8. [PubMed: 11846609]

28. Donner AJ, Szostek S, Hoover JM, Espinosa JM. CDK8 is a stimulus-specific positive coregulator of p53 target genes. Mol Cell 2007;27:121–33. [PubMed: 17612495]
29. Xu K, Ma H, McCown TJ, Verma IM, Kafri T. Generation of a stable cell line producing high-titer self-inactivating lentiviral vectors. Mol Ther 2001;3:97–104. [PubMed: 11162316]
30. Huang S, Liu LN, Hosoi H, Dilling MB, Shikata T, Houghton PJ. p53/p21(CIP1) cooperate in enforcing rapamycin-induced G(1) arrest and determine the cellular response to rapamycin. Cancer Res 2001;61:3373–81. [PubMed: 11309295]
31. Santos-Rosa H, Schneider R, Bannister AJ, et al. Active genes are tri-methylated at K4 of histone H3. Nature 2002;419:407–11. [PubMed: 12353038]
32. Jacobs JJ, Kieboom K, Marino S, DePinho RA, van Lohuizen M. The oncogene and Polycomb-group gene bmi-1 regulates cell proliferation and senescence through the ink4a locus. Nature 1999;397:164–8. [PubMed: 9923679]
33. Hendricks KB, Shanahan F, Lees E. Role for BRG1 in cell cycle control and tumor suppression. Mol Cell Biol 2004;24:362–76. [PubMed: 14673169]
34. Kang H, Cui K, Zhao K. BRG1 controls the activity of the retinoblastoma protein via regulation of p21CIP1/WAF1/SDI. Mol Cell Biol 2004;24:1188–99. [PubMed: 14729964]
35. Lee D, Kim JW, Seo T, Hwang SG, Choi EJ, Choe J. SWI/SNF complex interacts with tumor suppressor p53 and is necessary for the activation of p53-mediated transcription. J Biol Chem 2002;277:22330–7. [PubMed: 11950834]
36. Liu H, Kang H, Liu R, Chen X, Zhao K. Maximal induction of a subset of interferon target genes requires the chromatin-remodeling activity of the BAF complex. Mol Cell Biol 2002;22:6471–9. [PubMed: 12192045]
37. Gartel AL, Tyner AL. Transcriptional regulation of the p21((WAF1/CIP1)) gene. Exp Cell Res 1999;246:280–9. [PubMed: 9925742]
38. Ae K, Kobayashi N, Sakuma R, et al. Chromatin remodeling factor encoded by ini1 induces G1 arrest and apoptosis in ini1-deficient cells. Oncogene 2002;21:3112–20. [PubMed: 12082626]
39. Bracken AP, Kleine-Kohlbrecher D, Dietrich N, et al. The Polycomb group proteins bind throughout the INK4A-ARF locus and are disassociated in senescent cells. Genes Dev 2007;21:525–30. [PubMed: 17344414]
40. Roberts CW, Biegel JA. The role of SMARCB1/INI1 in development of rhabdoid tumor. Cancer Biol Ther 2009;8:412–6. [PubMed: 19305156]
41. Stojanova A, Penn LZ. The role of INI1/hSNF5 in gene regulation and cancer. Biochem Cell Biol 2009;87:163–77. [PubMed: 19234532]
42. Smith ME, Cimica V, Chinni S, Challagulla K, Mani S, Kalpana GV. Rhabdoid tumor growth is inhibited by flavopiridol. Clin Cancer Res 2008;14:523–32. [PubMed: 18223228]
43. Bourdeaut F, Freneaux P, Thuille B, et al. Extra-renal non-cerebral rhabdoid tumours. Pediatr Blood Cancer 2008;51:363–8. [PubMed: 18506766]
44. Molofsky AV, Pardal R, Iwashita T, Park IK, Clarke MF, Morrison SJ. Bmi-1 dependence distinguishes neural stem cell self-renewal from progenitor proliferation. Nature 2003;425:962–7. [PubMed: 14574365]
45. Zindy F, Quelle DE, Roussel MF, Sherr CJ. Expression of the p16INK4a tumor suppressor versus other INK4 family members during mouse development and aging. Oncogene 1997;15:203–11. [PubMed: 9244355]
46. Janzen V, Forkert R, Fleming HE, et al. Stem-cell ageing modified by the cyclin-dependent kinase inhibitor p16INK4a. Nature 2006;443:421–6. [PubMed: 16957735]
47. Cheng T, Rodrigues N, Shen H, et al. Hematopoietic stem cell quiescence maintained by p21cip1/waf1. Science 2000;287:1804–8. [PubMed: 10710306]
48. Kippin TE, Martens DJ, van der Kooy D. p21 loss compromises the relative quiescence of forebrain stem cell proliferation leading to exhaustion of their proliferation capacity. Genes Dev 2005;19:756–67. [PubMed: 15769947]
49. Chai J, Lu X, Godfrey V, et al. Tumor-specific cooperation of retinoblastoma protein family and Snf5 inactivation. Cancer Res 2007;67:3002–9. [PubMed: 17409406]

50. Ray A, Mir SN, Wani G, et al. hSNF5/INI1, a Component of the Human SWI/SNF Chromatin Remodeling Complex, Promotes Nucleotide Excision Repair by Influencing ATM Recruitment and Downstream H2AX Phosphorylation. Mol Cell Biol. 2009

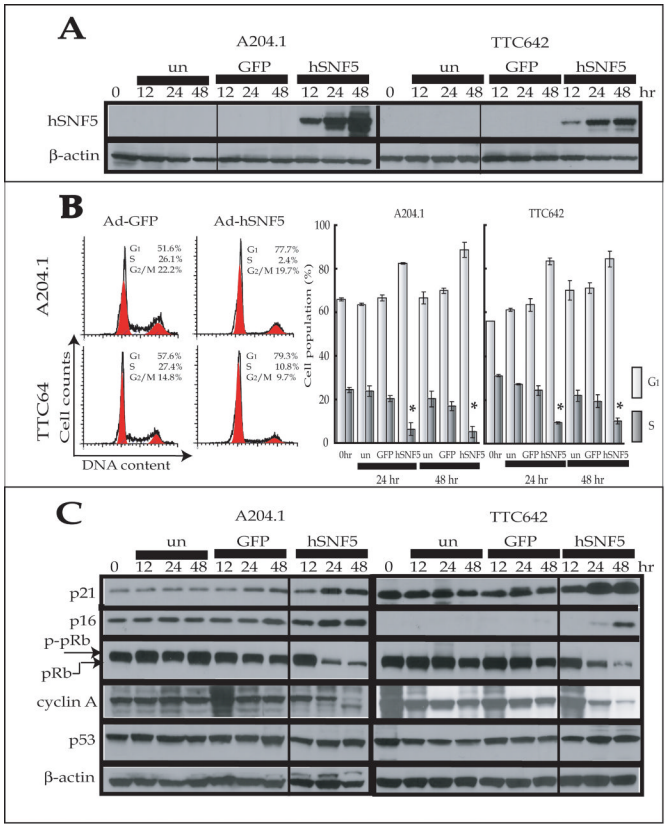

Figure 1. G_1 cell cycle arrest induced by reexpression of hSNF5

(A) Cells were harvested at the indicated times after infection with Ad-hSNF5 and Ad-GFP. Total cell protein (30 μg) were separated on a 4-20% SDS-polyacrylamide gel and probed with either anti-SNF5 or anti-ß-actin. un; uninfected control. (B) Twenty-four hours after infection with Ad-hSNF5 or Ad-GFP, cells were harvested and analyzed by flow cytometry. Left, representative profiles; Right, Values are the mean of three independent experiments; bars, ± SD. *, $P < 0.05$ relative to the number of S-phase of un-infection control. (C) Cells were harvested at the indicated times after infection with Ad-hSNF5 and Ad-GFP. Total cell protein (30 μg) were separated on a 4-20% SDS-polyacrylamide gel and probed with appropriate antibodies. un; uninfected control.

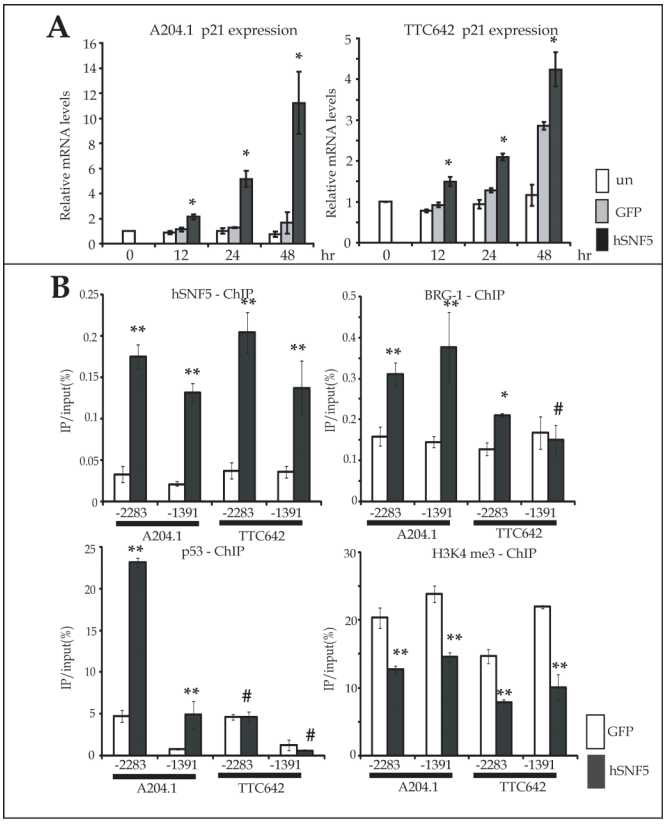

Figure 2. hSNF5-induced p21$^{CIP1/WAF1}$ expression

(A) RNA was extracted at the indicated times after infection with Ad-hSNF5 and Ad-GFP. The mRNA levels were measured for each gene by QT-PCR and normalized for β-actin expression. Values are the mean of three independent experiments; bars, ± SD. *, $P < 0.05$ relative to the Ad-GFP and un-infected control. un; uninfected control. (B) At 24 hours after infection with Ad-hSNF5 and Ad-GFP, protein was extracted for ChIPs assays. ChIPs assays were performed using antibodies directed against hSNF5, BRG-1, p53 and H3K4me3 on −2283 kb and −1391 kb of p21$^{CIP1/WAF1}$ promoter. Values are the mean of triplicates; bars, ± SD. *, $P < 0.05$ relative to the Ad-GFP control. **, $P < 0.01$ relative to the Ad-GFP control. #, $P > 0.05$ relative to the Ad-GFP control.

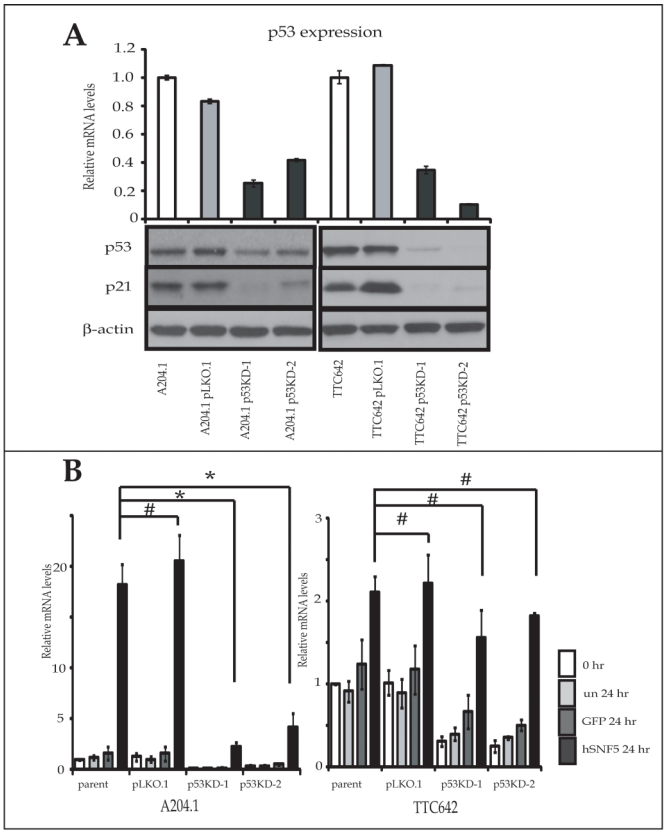

Figure 3. p21$^{CIP1/WAF1}$ expression after reexpression of hSNF5 in p53 stable knock down MRT cells

(A) p53 knock-down cells (A204 p53KD and TTC642 p53 KD) and the control cells (A204 pLKO.1 and TTC642 pLKO.1) were harvested and RNA and protein was extracted. The mRNA levels were measured by QT-PCR for each gene and normalized for β-actin expression. Values are the mean of three independent experiments; bars, ± SD. Total protein (30 μg) was separated on a 4-20% SDS-polyacrylamide gel and probed with appropriate antibodies. (B) Every 24 hours after infection with Ad-hSNF5 and Ad-GFP, cells were harvested and RNA was extracted. The mRNA levels were measured for each gene by QT-PCR and normalized for β-actin expression. Values are the mean of three independent experiments; bars, ± SD. *, $P < 0.05$ relative to the Ad-hSNF5 infected parent cells. #, $P > 0.05$ the Ad-hSNF5 infected parent cells.

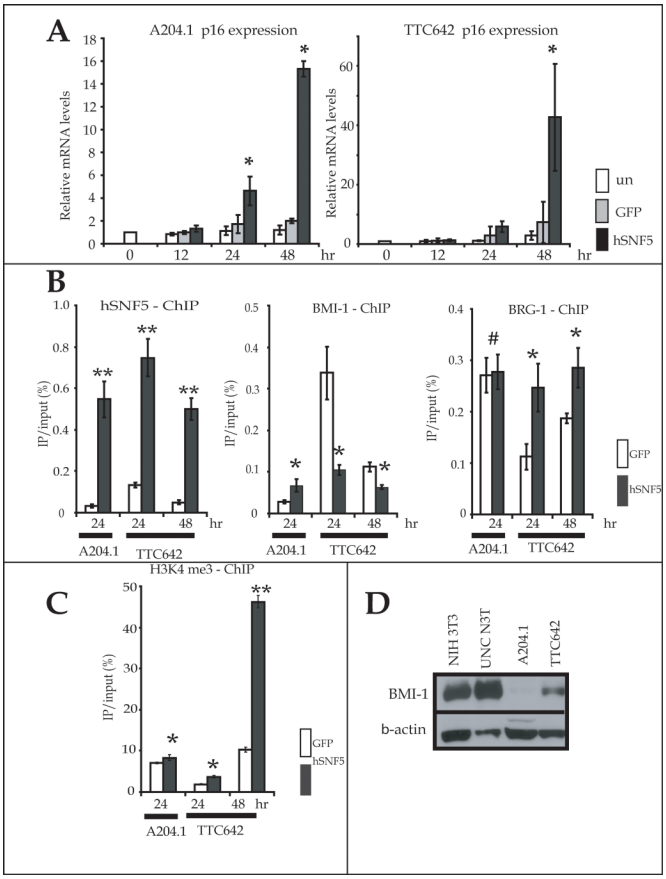

Figure 4. hSNF5-induced p16^{INK4A} expression

(A) Cells were infected with Ad-hSNF5 and Ad-GFP. RNA was extracted at the indicated times after infection. The mRNA levels were measured by QT-PCR analysis for each gene and normalized for β-actin expression. Values are the mean of three independent experiments; bars, ± SD. *, P < 0.05 relative to the Ad-GFP and un-infected control. un; uninfected control. (B, C) At 24 and 48 hours after infection with Ad-hSNF5 and Ad-GFP, cells were harvested and protein was extracted for ChIPs assays. ChIPs assays were performed using antibodies directed against hSNF5(B), BMI-1(B), BRG-1(B) and H3K4me3(C) on −450 kb site of p16^{INK4A} promoter. Values are the mean of triplicates; bars, ± SD. *, P < 0.05 relative to the Ad-GFP control. **, P < 0.01 relative to the Ad-GFP control. #, P > 0.05 relative to the Ad-GFP control. (D) Total protein (30 μg) were separated on a 4-20% SDS-polyacrylamide gel and probed with BMI-1 antibody.

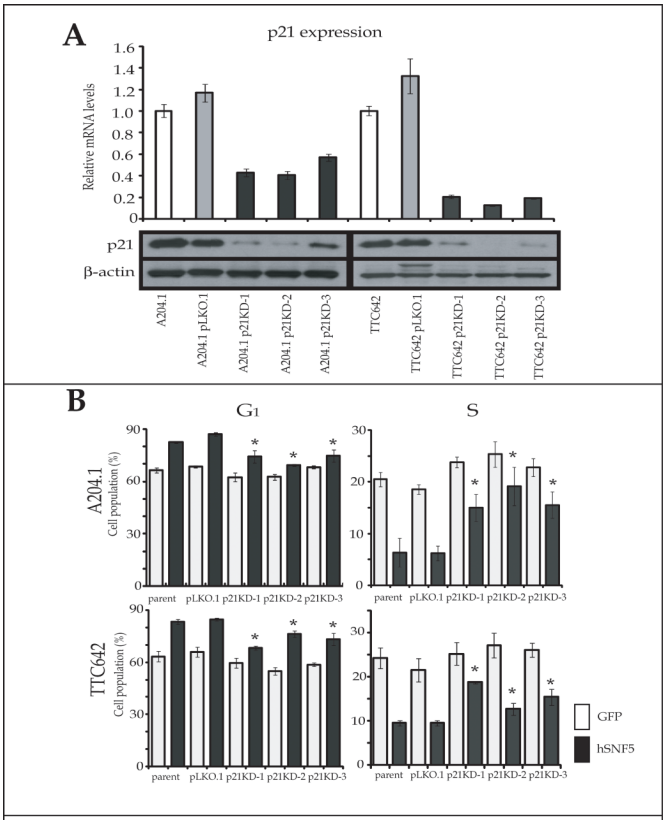

Figure 5. Inhibition of G_1 cell cycle arrest by reexpression of hSNF5 in $p21^{CIP1/WAF1}$ stable knock down MRT cells

(A) $p21^{CIP1/WAF1}$ knock-down cells (A204 p21KD and TTC642 p21 KD) and the control cells (A204 pLKO.1 and TTC642 pLKO.1) were harvested and RNA and protein was extracted. The mRNA levels were measured by QT-PCR for each gene and normalized for β-actin expression. Values are the mean of three independent experiments; bars, ± SD. Total protein (30 μg) was separated on a 4-20% SDS-polyacrylamide gel and probed with $p21^{CIP1/WAF1}$ antibodies. (B) Every 24 hours after infection with Ad-hSNF5 and Ad-GFP, cells were harvested and analyzed by flow cytometry. Values are the mean of three independent experiments; bars, ± SD. *, $P < 0.05$ relative to each Ad-GFP control.

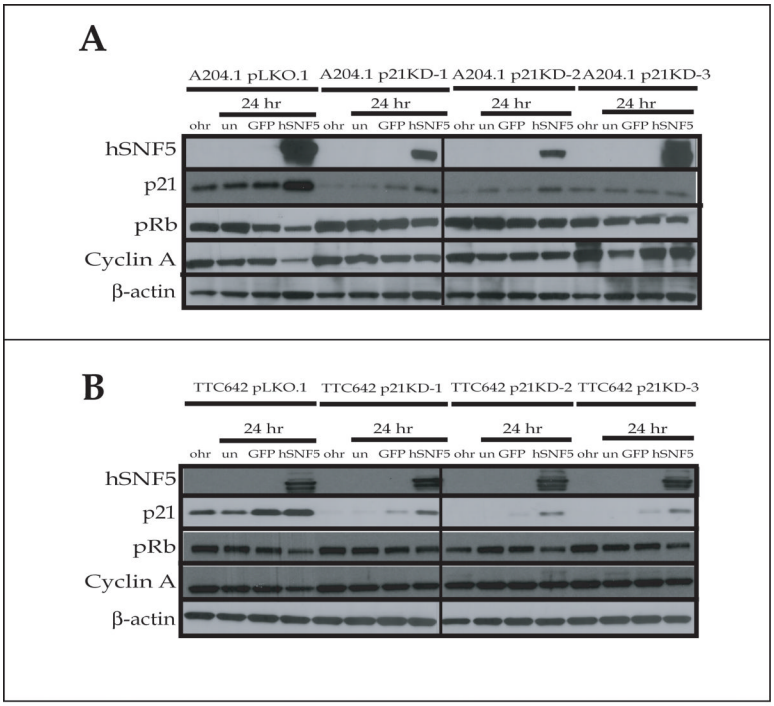

Figure 6. Inhibition of pRb dephosphorylation after hSNF5 reexpression in p21$^{CIP1/WAF1}$ knock-down MRT cell lines

(A, B) p21$^{CIP1/WAF1}$ knock-down cells (A204 p21KD and TTC642 p21 KD) and the control cells (A204 pLKO.1 and TTC642 pLKO.1) were harvested and protein was extracted. Total cell protein (30 μg) were separated on a 4-20% SDS-polyacrylamide gel and probed with appropriate antibodies.